

## Barrier Thickness Dependence of Photovoltaic Characteristics of InGaN/GaN Multiple Quantum Well Solar Cells

Noriyuki Watanabe<sup>1\*</sup>, Haruki Yokoyama<sup>1</sup>, Naoteru Shigekawa<sup>1†</sup>, Ken-ichi Sugita<sup>2</sup>, and Akio Yamamoto<sup>2</sup>

<sup>1</sup>NTT Photonics Laboratories, Nippon Telegraph and Telephone Corporation, Atsugi, Kanagawa 243-0198, Japan

<sup>2</sup>Graduate School of Engineering, University of Fukui, Fukui 910-8507, Japan

Received December 13, 2011; accepted June 5, 2012; published online October 22, 2012

We discuss the influence of the barrier thickness of an InGaN/GaN multiple quantum well (MQW) structure on solar cell performance. As barrier thickness decreases, short-circuit current density increases and open-circuit voltage decreases. The open-circuit voltage is much lower than expected from the absorption edge because of the large leakage current and large ideality factor of diodes owing to the carrier tunneling through the barrier. An MQW with a 3-nm-thick barrier layer shows a much longer carrier lifetime than that with a 9-nm-thick barrier layer. This is one possible reason for a higher short-circuit current in solar cell with the 3-nm-thick barrier MQW structure than that with the 9-nm-thick barrier MQW.

© 2012 The Japan Society of Applied Physics

### 1. Introduction

Group-III nitrides are attractive semiconductors for fabricating solar cells with high conversion efficiency. This is because the band gap of a ternary or quaternary compound can be set anywhere between 0.7 and 6.2 eV simply by changing the composition.<sup>1–3</sup> This band-gap range covers most of the solar spectrum. This means that the desired band gaps for subcells in a multijunction tandem solar cell can be easily obtained and the current-matching condition can be easily realized. These features are advantageous for the effective use of solar energy. Over the last five years, many investigations of InGaN-based solar cells have been reported.<sup>4–26</sup> However, their performance is still not nearly as high as expected. This is because it is very difficult to grow an InGaN layer with a suitable band-gap energy and with a sufficient crystal quality for achieving good photovoltaic performance. Therefore, many recent investigations have focused on improving the InGaN quality. For example, Kuwahara *et al.* reported that using a GaN substrate<sup>27</sup> and a multiple quantum well (MQW) structure<sup>28</sup> for InGaN-based solar cells is effective for improving the photovoltaic characteristics. In this study, we examine the influence of barrier layer thickness in the MQW absorption layers on the relationship between the photovoltaic behavior and crystal quality of InGaN/GaN MQW solar cells grown on GaN substrates by metal-organic chemical vapor deposition (MOCVD).

### 2. Experimental Procedure

Samples were grown on 2-in.-diameter n-type GaN free-standing substrates by MOCVD. The epitaxial layer structure is shown in Fig. 1. The barrier layer thickness was 3 or 9 nm. From the reciprocal space mapping of high-resolution X-ray diffraction, we confirmed that each epitaxial layer in the MQW structure was coherently grown on the GaN substrate. The optical band-gap energies of samples were evaluated by measuring absorption spectra at room temperature. The static photoluminescence (PL) was measured at room temperature using the excitation source of a He–Cd laser with an incident wavelength of 325 nm. The

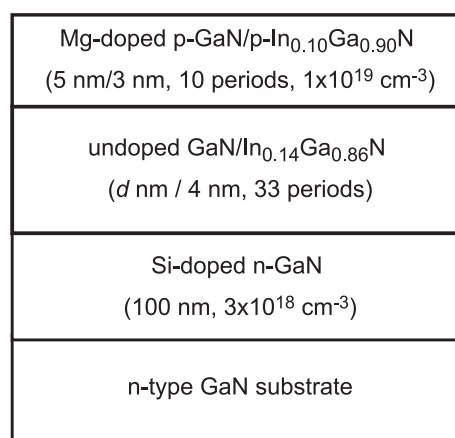


Fig. 1. Epitaxial layer structure of solar cells. The thickness of the barrier layer is 3 or 9 nm.

lifetime of photoinduced carriers was evaluated by measuring time-resolved PL (TRPL) spectra at room temperature using a laser diode with an incident wavelength of 375 nm as the excitation source.

Solar cells with dimensions of 2 × 2 mm<sup>2</sup> were fabricated on the whole two-inch wafer. The top surface of each cell was coated with an antireflection film. Fabricated solar cells were tested for photovoltaic characteristics. The current–voltage characteristics were measured under an air-mass 1.5 global (AM1.5G) illumination condition with a power density of 100 mW/cm<sup>2</sup>. Spectral responses of the solar cells were measured under a monochromatic illumination condition with a power density of 50 μW/cm<sup>2</sup>.

### 3. Results and Discussion

Figure 2 shows the voltage (*V*) dependence of the dark current density (*J*<sub>dark</sub>) of the fabricated solar cells without illumination. In the forward-bias region, the *J*<sub>dark</sub>–*V* curves of both cells have almost the same shape against the voltage, and the dark current shows single-exponential dependence on voltage until 1.5–2 V. Here, the turn-on voltage is defined as the voltage at which the current density reaches 0.01 mA/cm<sup>2</sup>. The deviation in the turn-on voltage is about 0.25 V smaller in the 3 nm barrier cell than in the 9 nm barrier cell. The ideality factor (*n*) derived from the slope of

\*E-mail address: watanabe.noriyuki@lab.ntt.co.jp

†Present address: Graduate School of Engineering, Osaka City University, Osaka 558-8585, Japan.

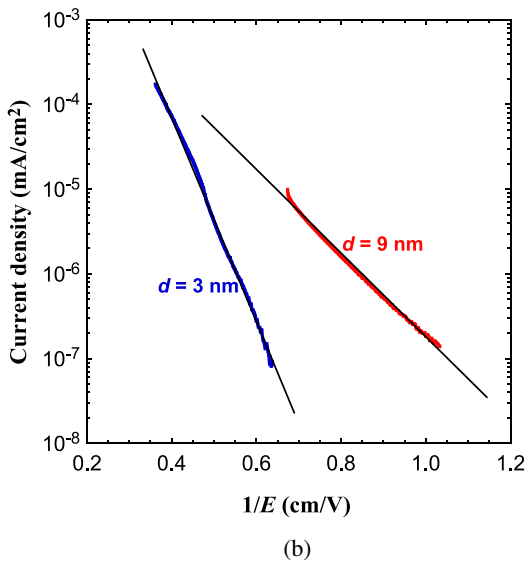
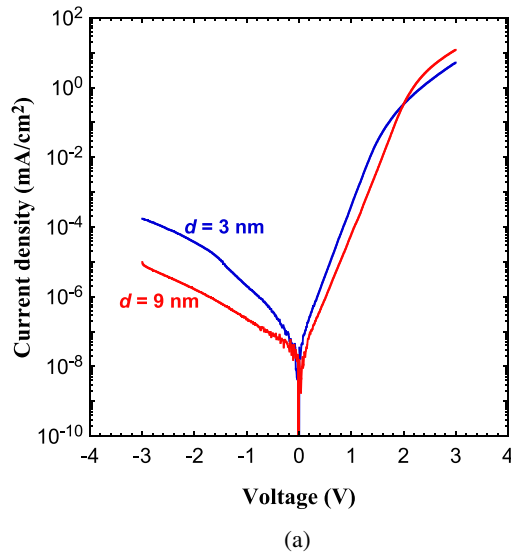


**Fig. 2.** (Color online) (a)  $J_{\text{dark}}-V$  curves of InGaN/GaN MQW solar cells with different barrier thicknesses without illumination. (b) The current density in the reverse bias region as a function of a reciprocal of an internal electric field under dark condition.

the curve is approximately  $n = 4.5$ . An ideality factor higher than  $n = 2$  might be caused by some tunnelling current<sup>29)</sup> through the barrier layers in the MQW structure. In the high-current region, the series resistance effect clearly appears. The 3 nm barrier cell shows the series resistance effect at approximately 1.4 V and the value of current density at 3 V is 5 mA/cm<sup>2</sup>. On the other hand, the 9 nm barrier cell does not show the series resistance effect until 2.0 V and its current density reaches 12 mA/cm<sup>2</sup>, which is over two times larger than that of the 3 nm barrier cell. These results suggest that the 3 nm barrier cell has a higher series resistance than the 9 nm barrier cell. In the reverse-bias region, the leakage current increases monotonically with increasing reverse bias. In Fig. 2(b), the leakage current in the reverse bias-region is plotted as a function of the reciprocal of the electric field  $E$ . Here,  $E$  is the sum of the applied field and the built-in field. The leakage currents of both cells show good exponential dependence on  $1/E$ . These results indicate that the leakage

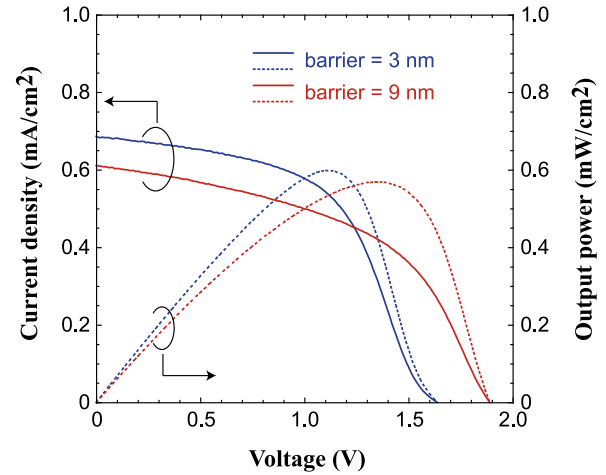


**Fig. 3.** (Color online)  $J-V$  and  $P-V$  curves of InGaN/GaN MQW solar cells with different barrier thicknesses under AM 1.5 illumination.

**Table I.** Solar cell parameters evaluated from Fig. 3.

	3 nm	9 nm
$J_{\text{SC}}$ (mA/cm <sup>2</sup> )	0.69	0.61
$V_{\text{OC}}$ (V)	1.64	1.89
FF (%)	53	49
$\eta$ (%)	0.60	0.57

current in the reverse-bias region is well described by a trap-assisted tunnelling (TAT) mechanism.<sup>30)</sup> The trap-assisted tunnelling current  $J_{\text{TAT}}$  is expressed as

$$J_{\text{TAT}} = A_{\text{TAT}} \exp\left(\frac{-8\pi\sqrt{2em^*}}{3hE} \varphi_r^{3/2}\right), \quad (1)$$

where  $A_{\text{TAT}}$  is a constant,  $m^*$  is the electron effective mass,  $e$  is the elementary charge,  $h$  is Planck's constant, and  $\varphi_r$  is the energy of the electron traps with respect to the conduction band edge. Assuming that the electron effective mass in the MQW is the same as that of GaN for both cells ( $0.2 m_0$ ), the trap energies are plausibly estimated to be 0.26 and 0.15 eV for the 3 and 9 nm barrier cells, respectively. This indicates that the electrons in the InGaN well easily move to the next well through the trap as a tunnelling current for the 3 nm barrier MQW.

Figure 3 shows the voltage dependence of the current density  $J$  and output power  $P$  of the fabricated solar cells of  $2 \times 2 \text{ mm}^2$  under AM1.5G illumination. Both solar cells show clear photovoltaic behavior under illumination. Solar cell parameters evaluated from the  $J-V$  curve and  $P-V$  curve are summarized in Table I. With a thinner barrier layer, the short-circuit current density  $J_{\text{SC}}$  increases and the open-circuit voltage  $V_{\text{OC}}$  decreases. The deviation in  $V_{\text{OC}}$  is equal to the difference in the turn-on voltage derived from the  $J_{\text{dark}}-V$  curves (Fig. 2). The fill factor ( $FF$ ) of both solar cells is approximately 50%, resulting in a similar maximum output power, that is, a similar conversion efficiency  $\eta$ . The slopes of the  $J-V$  curves near  $V = 0 \text{ V}$  (that is,  $J = J_{\text{SC}}$ ) are almost the same for the both cells, indicating that the shunt resistances are also the same for both cells. On the other hand, the slopes near  $J = 0 \text{ mA/cm}^2$  (that is,  $V = V_{\text{OC}}$ )

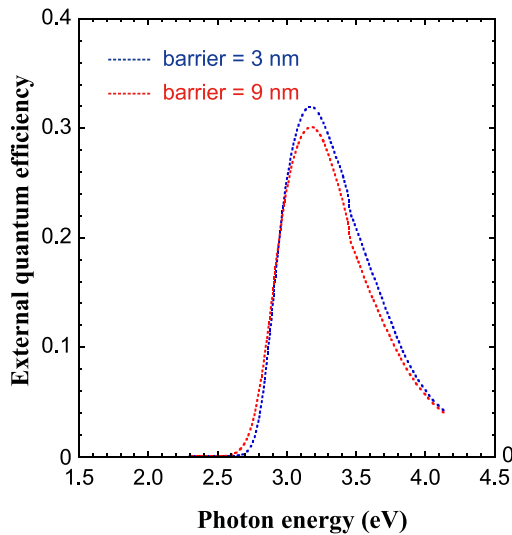


**Fig. 4.** (Color online) Spectral responses of InGaN/GaN MQW solar cells with different barrier thicknesses.

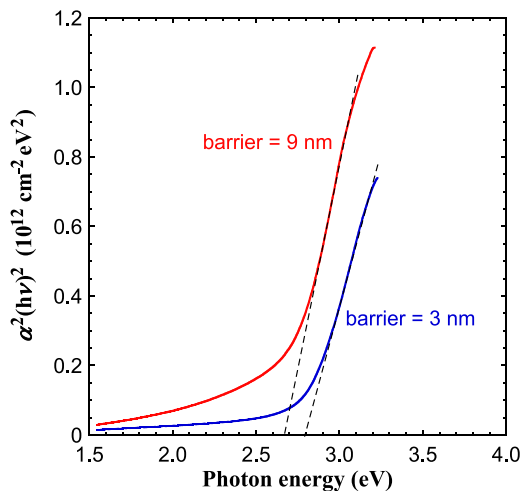


**Fig. 5.** (Color online) Optical absorption spectra of InGaN/GaN MQW solar cells with different barrier thicknesses.

become smaller than that at voltages less than  $V_{OC}$ . In particular, the variation in the slope for the 3 nm barrier cell is larger than that for the 9 nm barrier cell. This might be caused by the larger series resistance in the 3-nm-barrier cell, as shown in Fig. 2(a).

Figure 4 shows the spectral responses [the external quantum efficiency (EQE)] of the cells. The EQE spectra have almost the same shape against photon energy, and the maximum EQE value is about 30% at a photon energy of 3.2 eV. These results suggest that the values of the optical band gap  $E_g$  of the MQW absorption layers for both solar cells are quite similar. In fact, the absorption edge energies are 2.8 eV for the cell with the 3-nm-thick barrier and 2.7 eV for the cell with the 9-nm-thick barrier, as shown in Fig. 5. As GaN thickness increases under the same InGaN well layer, the internal electric field in the InGaN well increases. The increase in the internal electric field in the well layer should reduce the energy gap between the electron sub-band

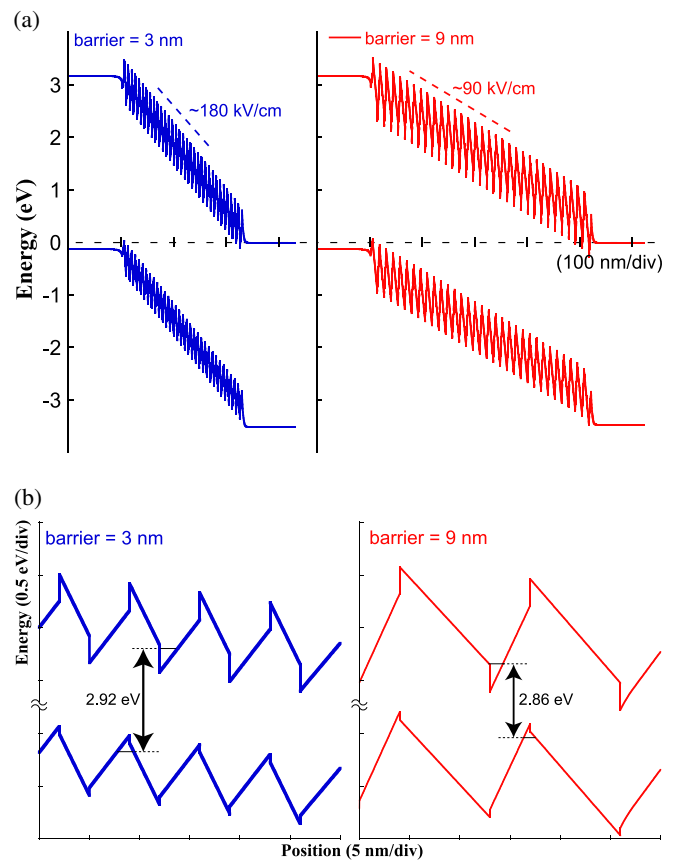


**Fig. 6.** (Color online) Band profiles of InGaN/GaN MQW solar cell structures shown in Fig. 1, calculated under the completely strained condition. (a) Whole-band profiles of solar cells; (b) enlargement of band profiles in MQW region.

and the heavy-hole sub-band, resulting in a decrease in absorption edge energy. Figure 6 shows the band profiles of the InGaN/GaN MQW solar cell structures shown in Fig. 1, calculated under the completely strained situation. From Fig. 6(b), the variation in the absorption edge between the 3 nm barrier MQW and the 9 nm barrier MQW is estimated to be 0.06 eV, which is quite similar to the deviation in absorption edge energy.

As is well known, the value of  $V_{OC}$  linearly depends on the band-gap energy, as expressed by the following empirical relationship:

$$V_{OC} = \frac{E_g}{e} - 0.4, \quad (2)$$

where  $E_g$  is the band-gap energy. From the absorption spectra (Fig. 5), the band-gap energy of the MQW absorption layer was determined to be in the range of 2.7–2.8 eV. Therefore, according to eq. (2),  $V_{OC}$  should be 2.3–2.4 V, which is much larger than the experimental values. There could be several reasons for the reduction in open-circuit voltage. For example, the influence of the leakage current in the reverse-bias region is one possibility. A higher saturation current makes the open-circuit voltage low. As shown in the  $J_{dark}$ - $V$  curves (Fig. 2), both cells show the TAT-type leakage current. It could be roughly approximated that this type of leakage current linearly depends on the exponential

of the reverse bias voltage in the high-bias region. This property has the same effect as the saturation current increases, that is, reduction in  $V_{OC}$ . Additionally, a turn-on voltage under the high ideality factor properties lower than the value expected from  $E_g$  is another possible reason for the low  $V_{OC}$ . As described above, the forward current might be limited by the tunnelling current through the GaN barrier layer. This would explain why the ideality factor is very large and the turn-on voltage becomes low. The tunnelling current through the GaN barrier decreases the effective  $E_g$ , resulting in the reduction in  $V_{OC}$ .

The value of  $J_{SC}$  is approximately given as follows:

$$J_{SC} = e \cdot C \int_0^\infty F(\lambda)[1 - \exp(-\alpha(\lambda) \cdot w)] d\lambda, \quad (3)$$

where  $F(\lambda)$  is the solar spectrum,  $\alpha(\lambda)$  is the absorption coefficient,  $w$  is the effective thickness of the absorption layer, and  $C$  is the collection efficiency. For  $C = 1$ , eq. (3) gives the maximum short-circuit current density ( $J_{SC-max}$ ) of a solar cell that has an absorption layer with the thickness  $w$  and absorption coefficient  $\alpha(\lambda)$ . From eq. (3) and Fig. 5, the value of  $J_{SC-max}$  should be higher in the 9-nm-barrier cell. The actual  $J_{SC}$  of the 9-nm-barrier cell, however, is lower. This indicates that the collection efficiency of the 3-nm-barrier cell should be higher than that of the 9-nm-barrier cell. Some of the photoinduced carriers in the MQW absorption layer diffuse or drift in the MQW layer and collect into the n-type (electrons) or p-type (holes) contact layer. These carriers are observed as current. In the p-i-n type cell, as shown in Fig. 1, the drift process is dominant and the drift probability should increase as the slope of the band profile as the intrinsic layer increases, resulting in the larger current. As shown in Fig. 6(a), the slope of the band profile in the MQW region is estimated to be about 180 kV/cm for the 3 nm barrier MQW and about 90 kV/cm for the 9 nm barrier MQW; that is, the slope of the band profile of the 3 nm barrier MQW is about two times larger. This may be one of the reasons for the higher collection efficiency, or  $J_{SC}$ , in the 3-nm-thick barrier solar cell. The lifetime of photoinduced carriers might also be correlated with the short-circuit current. The TRPL profiles of the two solar cells measured at room temperature [Fig. 7(a)] indicate that the carrier lifetime of the 3 nm barrier cell is much longer than that of the 9 nm barrier cell. Additionally, from a comparison between the PL spectra [Fig. 7(b)] and the absorption spectra (Fig. 5), one can see that the PL peak energy of the 3-nm-barrier cell (2.3 eV) is smaller than the absorption edge energy (2.8 eV), while the PL peak energy and the absorption edge energy of the 9 nm barrier is nearly the same (2.6–2.7 eV). These results suggest that the radiative recombination process is different between the two samples, and this difference in the radiative recombination process might result in the difference in the lifetime of the photoinduced carriers. This difference in the radiative recombination process might influence short-circuit current. Further investigations are needed to clarify the correlation between photoinduced carrier lifetime and short-circuit current.

#### 4. Conclusion

We investigated the influence of the barrier thickness of an InGaN/GaN MQW structure on solar cell performance. As

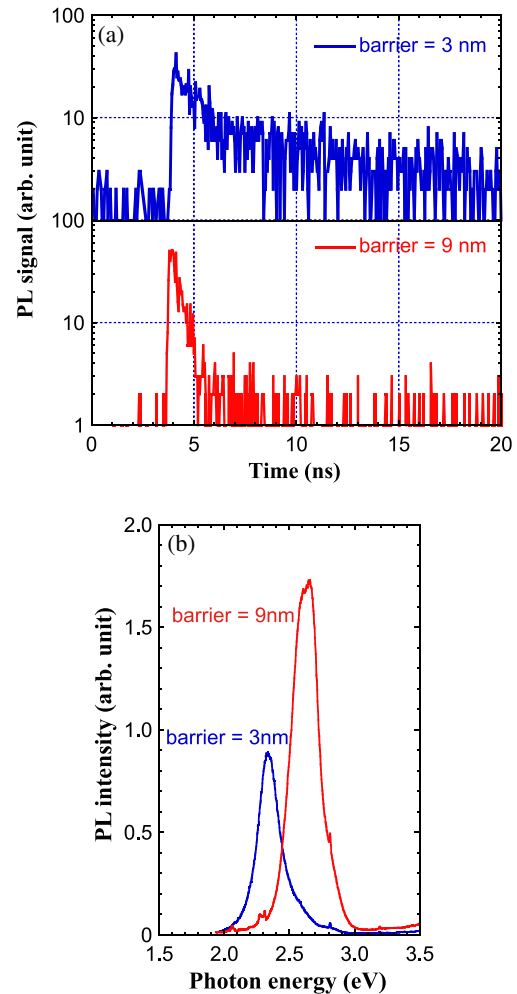


**Fig. 7.** (Color online) (a) Decay curves of total PL intensity and (b) static PL spectra of InGaN/GaN MQW solar cells with different barrier thicknesses measured at room temperature.

barrier thickness decreases, short-circuit current density increases and open-circuit voltage decreases. From the analysis of the  $J_{dark}-V$  curve, the trap-assisted tunneling current is dominant in the reverse leakage current and the trap energy is larger for a 3-nm-thick barrier MQW than a 9-nm-thick barrier MQW. These results suggest that open-circuit voltage is lower than expected from absorption edge energy and that open-circuit voltage decreases as barrier thickness decreases. The MQW with the 3-nm-thick barrier layer shows a much longer carrier lifetime at room temperature than that with the 9-nm-thick barrier layer. The longer carrier lifetime might result in the higher short-circuit current density.

#### Acknowledgements

The authors are indebted to Dr. Tomoyuki Akeyoshi and Dr. Takatomo Enoki for their continuous encouragement. This work was supported in part by the “Creative research for clean energy generation using solar energy” project in the Core Research for Evolutional Science and Technology (CREST) programs of the Japan Science and Technology Agency (JST).

- 1) J. Wu, W. Walukiewicz, K. M. Yu, J. W. Ager III, E. E. Haller, H. Lu, and W. J. Schaff: *Appl. Phys. Lett.* **80** (2002) 4741.
- 2) W. Walukiewicz, S. X. Li, J. Wu, K. M. Yu, J. W. Ager III, E. E. Haller, H. Lu, and W. J. Schaff: *J. Cryst. Growth* **269** (2004) 119.
- 3) R. E. Jones, R. Broesler, K. M. Yu, J. W. Ager III, E. E. Haller, W. Walukiewicz, X. Chen, and W. J. Schaff: *J. Appl. Phys.* **104** (2008) 123501.
- 4) A. Yamamoto, Md. R. Islam, T.-T. Kang, and A. Hashimoto: *Phys. Status Solidi C* **7** (2010) 1309.
- 5) O. Jani, I. Ferguson, C. Honsberg, and S. Kurtz: *Appl. Phys. Lett.* **91** (2007) 132117.
- 6) C. J. Neufeld, N. G. Toledo, S. C. Cruz, M. Iza, S. P. DenBaars, and U. K. Mishra: *Appl. Phys. Lett.* **93** (2008) 143502.
- 7) X. Zheng, R. H. Horng, D. S. Wu, M. T. Chu, W. Y. Liao, M. H. Wu, R. M. Lin, and Y. C. Lu: *Appl. Phys. Lett.* **93** (2008) 261108.
- 8) J. K. Sheu, C. C. Yang, S. J. Tu, K. H. Chang, M. L. Lee, W. C. Lai, and L. C. Peng: *IEEE Electron Device Lett.* **30** (2009) 225.
- 9) S. W. Zeng, B. P. Zhang, J. W. Sun, J. F. Cai, C. Chen, and J. Z. Yu: *Semicond. Sci. Technol.* **24** (2009) 055009.
- 10) R. H. Horng, S. T. Lin, Y. L. Tsai, M. T. Chu, W. Y. Liao, M. H. Wu, R. M. Lin, and Y. C. Lu: *IEEE Electron Device Lett.* **30** (2009) 724.
- 11) X. M. Cai, S. W. Zeng, and B. P. Zhang: *Appl. Phys. Lett.* **95** (2009) 173504.
- 12) M. J. Jeng, Y. L. Lee, and L. B. Chang: *J. Phys. D* **42** (2009) 105101.
- 13) R. Dahal, B. Pantha, J. Li, J. Y. Lin, and H. X. Jiang: *Appl. Phys. Lett.* **94** (2009) 063505.
- 14) C. L. Tsai, G. S. Liu, G. C. Fan, and Y. S. Lee: *Solid-State Electron.* **54** (2010) 541.
- 15) S. W. Zeng, X. M. Cai, and B. P. Zhang: *IEEE J. Quantum Electron.* **46** (2010) 783.
- 16) J. J. Wierer, A. J. Fischer, and D. D. Koleske: *Appl. Phys. Lett.* **96** (2010) 051107.
- 17) K. Y. Lai, G. J. Lin, Y.-L. Lai, Y. F. Chen, and J. H. He: *Appl. Phys. Lett.* **96** (2010) 081103.
- 18) I. M. Pryce, D. D. Koleske, A. J. Fischer, and H. A. Atwater: *Appl. Phys. Lett.* **96** (2010) 153501.
- 19) B. R. Jampana, A. G. Melton, M. Jamil, N. N. Faleev, R. L. Opila, I. T. Ferguson, and C. B. Honsberg: *IEEE Electron Device Lett.* **31** (2010) 32.
- 20) M. J. Jeng, T. W. Su, Y. L. Lee, Y. H. Chang, L. B. Chang, R. M. Lin, J. H. Jiang, and Y. C. Lu: *Jpn. J. Appl. Phys.* **49** (2010) 052302.
- 21) R. H. Horng, M. T. Chu, H. R. Chen, W. Y. Liao, M. H. Wu, K. F. Chen, and D. S. Wu: *IEEE Electron Device Lett.* **31** (2010) 585.
- 22) C. C. Yang, J. K. Sheu, X. W. Liang, M. S. Huang, M. L. Lee, K. H. Chang, S. J. Tu, F. W. Huang, and W. C. Lai: *Appl. Phys. Lett.* **97** (2010) 021113.
- 23) R. Dahal, J. Li, K. Aryal, J. Y. Lin, and H. X. Jiang: *Appl. Phys. Lett.* **97** (2010) 073115.
- 24) J. P. Shim, S. R. Jeon, Y. K. Jeong, and D. S. Lee: *IEEE Electron Device Lett.* **31** (2010) 1140.
- 25) H. C. Lee, Y. K. Su, W. H. Lan, J. C. Lin, K. C. Huang, W. J. Lin, Y. C. Cheng, and Y. H. Yeh: *IEEE Photonics Technol. Lett.* **23** (2011) 347.
- 26) J. R. Lang, C. J. Neufeld, C. A. Hurmi, S. C. Cruz, E. Matioli, U. K. Mishra, and J. S. Speck: *Appl. Phys. Lett.* **98** (2011) 131115.
- 27) Y. Kuwahara, T. Fujii, Y. Fujiyama, T. Sugiyama, M. Iwaya, T. Takeuchi, S. Kamiyama, I. Akasaki, and H. Amano: *Appl. Phys. Express* **3** (2010) 111001.
- 28) Y. Kuwahara, T. Fujii, T. Sugiyama, D. Iida, Y. Isobe, Y. Fujiyama, Y. Morita, M. Iwaya, T. Takeuchi, S. Kamiyama, I. Akasaki, and H. Amano: *Appl. Phys. Express* **4** (2011) 021001.
- 29) X. A. Cao, E. B. Stokes, P. M. Sandvik, S. F. LeBoeuf, J. Kretchmer, and D. Walker: *IEEE Electron Device Lett.* **23** (2002) 535.
- 30) R. Mahapatra, A. K. Chakraborty, N. Poolamai, A. Horsfall, S. Chattopadhyay, N. G. Wright, K. S. Coleman, P. G. Coleman, and C. P. Burrows: *J. Vac. Sci. Technol. B* **25** (2007) 217.